https://doi.org/10.5194/egusphere-2026-4423
Preprint. Discussion started: 28 July 2026

Photochemical ageing drives the browning of urban outflows through secondary brown carbon production

Alejandra Velazquez-Garcia[1], Chenjie Yu[2], Sarah Tinorua[1*], Hichem Bouzidi [2], Eleonora Aruffo[3], Piero Di Carlo[4], Peter DeCarlo[5], Benjamin A. Nault[5,6,7], Thierry Bourrianne[1], Kevin Tu[2**], Edouard Pangui[2], Diana L. Pereira[2***], Mathieu Cazaunau[2], Ludovico Di Antonio[8****], Guillaume Siour[8], Matthias Beekmann[2], Astrid Bauville[2*****], Christopher Cantrell[8], Paola Formenti[2], Vincent Michoud[2] and Cyrielle Denjean[1].

[1]Météo-France, CNRS, Univ. Toulouse, CNRM, Toulouse, France
[2]Université Paris Cité et Univ Paris Est Creteil, CNRS, LISA, F-75013, Paris, France.
[3]University "G. d'Annunzio" of Chieti-Pescara, Department of Science, Center for Advanced Studies and Technology (CAST), Chieti, Italy
[4]University "G. d'Annunzio" of Chieti-Pescara, Department of Advanced Technologies in Medicine & Dentistry (DTM&O), Center for Advanced Studies and Technology (CAST), Chieti, Italy
[5]Department of Environmental Health and Engineering, Johns Hopkins University, Baltimore, United States
[6]Institute for Planetary Health, Johns Hopkins University, Baltimore, United States
[7]Center for Aerosol and Cloud Chemistry, Aerodyne Research, Inc., Billerica, United States
[8]Université Paris Est Creteil et Université Paris Cité, CNRS, LISA, F-94100, Creteil, France.
[*]now at Institute of Applied Geosciences, Technical University Darmstadt, Darmstadt, Germany
[**]now at Safran Aircraft Engines/Akkodis, 77550 Moissy-Cramayel, France.
[***]now at Institute for Atmospheric and Earth System Research / Physics, Faculty of Science, University of Helsinki, Helsinki, 00014, Finland
[****]now at LATMOS/IPSL, Sorbonne Université, UVSQ, CNRS, 75252 Paris, France
[*****]now at Muséum national d'Histoire naturelle (MNHN, CNRS), BioArch, Paris

Correspondence to: Alejandra Velazquez-Garcia (ale-vg13@hotmail.com) and Cyrielle Denjean (cyrielle.denjean@meteo.fr)

Abstract. Brown carbon (BrC) absorbs solar radiation, thereby partially offsetting the cooling effect of aerosols on the climate. However, its contribution to climate forcing remains poorly constrained and is currently not explicitly included in the overall radiative forcing estimates of the IPCC. In this work, we quantify the contributions of BrC to light absorption in urban outflows from Paris using aircraft observations. We observe a progressive "browning" of the plume over 6 hours of transport time, characterised by a significant increase in the relative contribution of BrC to aerosol light absorption. This optical shift is strongly correlated with photochemical ageing as evidenced by the increase in the organic aerosols-to-BC mass ratio and the simultaneous depletion of aromatic volatile organic precursors. The corresponding rise in the Absorption Angström Exponent from 1.1 to 2.6 provides further evidence that secondary organic aerosol formation is the primary driver of enhanced light absorption at 450 nm in the aged plume. Our observations indicate that BrC is photochemically produced during transport at a rate of ~ 0.25 h^{-1} over 6 hours of atmospheric processing under the conditions examined in this study. For these cases, the findings suggest that urban outflows are not merely diluted during transport but undergo significant

https://doi.org/10.5194/egusphere-2026-4423
Preprint. Discussion started: 28 July 2026

chemical transformations that alter their radiative impact. Accounting for these time-dependent optical changes provides a way to refine how climate models simulate radiative impacts of large metropolitan areas to climate change.

1 Introduction

Light-absorbing carbonaceous aerosols (LACs) partially offset the overall climate-cooling of aerosols. They comprise black carbon (BC) and brown carbon (BrC), a part of organic aerosol (OA), which absorbs sunlight and has a strong spectral dependence, especially at ultraviolet and short visible wavelengths (Laskin et al., 2015; Saleh et al., 2014; Kirchstetter et al., 1999). They exert a positive radiative forcing and thereby warm the atmosphere through direct absorption, reducing the snow/ice albedo, altering planetary boundary height, and modifying the cloud formation and global precipitation patterns (Bond and Bergstrom, 2006). Legislative efforts to reduce anthropogenic emissions have been implemented globally (Kaskaoutis et al., 2023). However, the radiative influence of LACs aerosols has increased over the past two decades (Li et al., 2022). Robust projections of climate change in response to future LACs emissions and associated global warming remain both a challenge for the scientific community and an important topic at the science-policy interface (Gliß et al., 2021; Samset et al., 2018; Szopa et al., 2023).

The contribution of BrC to climate forcing is poorly constrained, leading to a wide range of estimated direct radiative effects (+0.04 to +0.57 W m^{-2}). Wang et al. (2018) suggested that direct radiative forcing of BrC is overestimated due to the bias between observations and simulations. Indeed, this uncertainty reflects both the diversity of the representation of BrC in atmospheric models and the limited understanding of its chemical and optical properties during its full atmospheric lifecycle, from emission to evolution during transport (Drugé et al., 2022). In addition, direct observations constraining the key processes throughout the lifecycle of ambient BrC remain limited.

Primary BrC is usually associated with biomass combustion, while fossil-fuel combustion is typically a minor contributor, except for specific sources such as low-efficiency residential coal combustion and heavy fuel oil use in ship engines (Andreae and Gelencsér, 2006; Desyaterik et al., 2013; Feng et al., 2013; Washenfelder et al., 2015; Zhang et al., 2017; Corbin et al., 2018, 2019; Xie et al., 2019; Saleh, 2020). Secondary BrC can also be produced from the photo-oxidation of volatile organic compounds (VOCs) through reactions occurring in the gas phase (Jacobson, 1999; Laskin et al., 2015; Moise et al., 2015; Nakayama et al., 2013; Saleh et al., 2013; Sareen et al., 2013). Previous laboratory and ambient studies present contrasting BrC lifetimes, ranging from a few hours (Hems and Abbatt, 2018; Zhao et al., 2015; Zhong and Jang, 2014), to 13 – 28 hours (Forrister et al., 2015; Velazquez-Garcia et al., 2024; Wong et al., 2019; Yu et al., 2026a), or even 22 – 45 hours (Wang et al., 2016) after emission, likely reflecting differences in BrC sources, chemical composition, and atmospheric ageing processes.

https://doi.org/10.5194/egusphere-2026-4423
Preprint. Discussion started: 28 July 2026

Various chemical transformations contributing to secondary BrC formation have been reported. Although BrC has been observed in biogenic secondary OA (SOA) formed in the presence of ammonia (Flores et al., 2014; Lee et al., 2014), the resulting absorption is considerably weaker than that arising from the oxidation of aromatic VOCs precursors, which are generally linked to combustion emissions (Zhang et al., 2011; Nakayama et al., 2013; Zhong and Jang, 2014; Liu et al., 2015; Moise et al., 2015; Dingle et al., 2019; Saleh, 2020). For example, Zhang et al. (2011) reported 4 to 6 times higher SOA absorption in anthropogenically dominated environment by aromatic VOCs (e.g., Los Angeles, California) than in a mixed anthropogenic-biogenic environment (e.g., Atlanta, Georgia). Consistent with these findings, laboratory studies have shown that SOA formed from the oxidation of anthropogenic aromatic precursors, including naphthalene, toluene, and m-xylene, exhibits significant light-absorbing properties (Liu et al., 2015; Nakayama et al., 2013). Such observations suggest an important role of anthropogenic photochemical processing in secondary BrC formation, particularly in urban environments.

As BrC is not chemically stable, it may experience rapid photobleaching during atmospheric transport, which reduces its absorption properties over time, thereby modulating its contribution to aerosol radiative forcing (Wong et al., 2017; Zhao et al., 2015). For a subset of BrC biomass burning species, Zhao et al. (2015) reported photo-enhancement and photobleaching changes in rapid timescales, i.e., on the order of an hour or less. Wang et al. (2019) observed over the southeastern margin of Tibetan Plateau a diurnal cycle in secondary BrC, characterised by photochemical oxidation after sunrise followed by photobleaching of the chromophores under increasingly oxidising conditions as the day progressed. From an analysis of satellite observations and chemistry-transport modelling, Konovalov et al. (2021) showed for a Siberian fire plume that its absorption decreased due to photobleaching in the first hours after emission and then increased to a certain degree due to secondary BrC build-up. In Paris, active summertime photochemistry has been associated with an increasing contribution of BrC to aerosol light absorption (Navarro-Barboza et al., 2025; Di Antonio et al., 2025a; Yu et al., 2026a).

Aircraft observations from the ACROSS (Atmospheric ChemistRy Of the Suburban foreSt) campaign have provided insights into the atmospheric processing of LACs within the Paris urban plume. These studies revealed that plume ageing alters aerosol optical properties through enhanced BC light absorption driven by non-BC components (Velazquez-Garcia et al., 2026a) and through SOA formation associated with an increasing contribution of BrC to light absorption (Yu et al., 2026b). These observations motivate further investigation of the coupling between BrC optical properties, SOA formation, and atmospheric oxidation during plume transport to better understand BrC ageing under ambient conditions. Building upon these findings, the present study investigates these coupled processes, providing observational constraints on the factors controlling BrC optical evolution during atmospheric ageing. While laboratory studies provide important mechanistic insights, semi-Lagrangian aircraft observations tracking plume evolution enable the investigation of these processes under complex ambient atmospheric conditions. By combining chemical and optical measurements, as well as atmospheric transport simulations, we aim to: (1) characterise the contribution of BrC to aerosol absorption; (2) investigate the effects of

https://doi.org/10.5194/egusphere-2026-4423
Preprint. Discussion started: 28 July 2026

atmospheric transport and photochemical ageing on BrC; (3) provide recommendations for incorporating BrC dynamics into climate models.

2 Methods

The ACROSS field campaign integrated coordinated aircraft and ground-based observations, aiming to study at different distances the urban plume emitted from Paris, particularly when they encounter air masses influenced by biogenic emissions from the surrounding forests (Cantrell and Michoud, 2022). Airborne measurements utilised in this work were conducted aboard the French ATR42 environmental research aircraft operated by Safire (the French aircraft service for environmental research) over Paris and its surrounding areas from June 21 to July 5, 2022. Stationed at the Cergy aerodrome (34 km from Paris centre), the aircraft performed a series of 15 scientific flights across northwestern France, specifically within a region bounded between 47.5° and 50.5° to the north and -1° to -5° to the east. For the 15-flight ensemble, urban plumes were sampled at downwind distances ranging from a few kilometres to ~200 km.

2.1 Aircraft measurements

Aerosol particles were collected using the AVIRAD aerosol inlet system (Formenti et al., 2011), which consists of an isokinetic and isoaxial inlet mounted beneath the aircraft. The inlet provides a 50% transmission efficiency for particles with diameters up to 12 µm (Denjean et al., 2016). Multiple sampling lines distribute the aerosol flow to instruments dedicated to measuring aerosol concentrations and their physicochemical properties. The gas-phase measurements were sampled through a pressurised manifold. All results presented in this study are reported under standard temperature and pressure conditions (T=273.15 K, P = 1013,25 hPa).

The aerosol scattering (σ_{scatt}) and extinction (σ_{ext}) coefficients at 450 and 630 nm were obtained with an Aerosol Absorption Spectral Sizer (A2S2), an adapted airborne version of a dual-wavelength cavity-attenuated phase-shift ($CAPS_{PMSSA}$, Aerodyne Inc. Billerica, MA, USA) instrument (Yu et al., 2024). The scattering channels of the A2S2 were calibrated using nebulized 200 nm polystyrene latex (PSL) spheres. Following (Yu et al., 2024), the measured scattering coefficients were corrected for angular truncation effects, with mean correction factors of 1.13 at 450 nm and 1.05 at 630 nm applied under the ACROSS campaign conditions.

The BC-containing particles were measured by a Single-Particle Soot Photometer (SP2; Droplet Measurement Technologies, Longmont, CO, USA) to assess BC properties such as, mass concentration, size distribution, and mixing state (Laborde et al., 2012; Moteki and Kondo, 2010; Schwarz et al., 2008; Subramanian et al., 2010). The SP2 measures the incandescence signal of individual particles within the 90-580 nm particle diameter range. The mass of BC cores is derived from the incandescence signal using a calibration factor obtained by measuring the incandescence peak height of sizes selected

https://doi.org/10.5194/egusphere-2026-4423
Preprint. Discussion started: 28 July 2026

fullerene soot (Alfa Aesar, lot no. FS12S011). The SP2 data were processed using the SP2PyPro toolkit (Tinorua et al., 2024; Velazquez-Garcia et al., 2026b).

The sub-micron non-refractory aerosol composition and concentration was characterised using a mini-Aerosol Mass Spectrometer (mAMS; Aerodyne Inc., Billerica, Ma, USA) (Drewnick et al., 2005; Konwar et al., 2024; Vu et al., 2016). This instrument provides quantitative information on organic and inorganic aerosol components, including sulphate, ammonium, nitrate, and chloride. Instrument calibration involved determining the ionization efficiency with monodisperse ammonium nitrate particles, while a fixed collection efficiency of 0.5 has been used. The experimental configuration and data treatment are described in detail in Yu et al. 2026b.

The VOCs (including benzene, toluene, C8 aromatics) were measured with an adapted airborne version of a high-resolution proton-transfer-reaction time-of-flight mass spectrometer (HR-PTR-ToF-MS, manufactured by Kore Technology Ltd.), as described in detail by Michoud, V. and Bouzidi, H. (2024). Blank measurements were conducted once on the ground before the flight, or twice before and after the flight. Regular calibrations were performed before each flight using gaseous VOC standards from a certified calibration mixing provided by the National Physical Laboratory (NPL) and a dilution system. Sensitivity determined from calibration, corrected for humidity variations, was used to retrieve the volume mixing ratios of targeted VOCs. The limit of detection was calculated based on a signal-to-noise ratio of 3 over a period of 10 minutes.

Ozone (O_3) was measured using a Thermo Environmental Instruments TEI 49i TL analyser based on UV photometry. The O_3 data was processed and validated according to the standards of the MOZAIC-IAGOS (Measurements of OZone, water vapour, carbon monoxide and nitrogen oxides by in-service AIrbus airCraft) programme. NO_2 was measured using a four-channel thermal dissociation-laser induced fluorescence (TD-LIF) instrument employing a pulsed YAG-laser emitting light at 532 nm (Di Carlo et al., 2013). Calibrations were performed before and after each flight, using NO_2 and zero air standard cylinders. Carbon monoxide (CO) was sampled using a PICARRO analyser (model G2401) which is based on cavity ring-down spectroscopy (CRDS) technology. Calibration was carried out before and after each campaign, with a target control gas being passed at the beginning and at the end of each flight. The data were processed and validated according to the ICOS (Integrated Carbon Observation System) research infrastructure protocols (Filges et al., 2015).The number of data points for each instrument and flight is provided in the supplementary information (Table S1).

2.2 Additional model products

A regional 3D simulation was performed using the WRF-CHIMERE v2020r3 chemical transport model (Menut et al., 2021), covering the Paris area at a horizontal resolution of 2 km and with 10 vertical layers extending from the surface to 500 hPa (Di Antonio et al., 2025b). The model simulates transport pathways of emissions including gas and aerosols concentrations, while taking into account meteorological variables from the WRF model. The simulation covered the period from June 15 to

https://doi.org/10.5194/egusphere-2026-4423
Preprint. Discussion started: 28 July 2026

July 25, 2022, including a two-week model spin-up period. Anthropogenic emissions, including BC, were taken from the CAMS-GLOB-ANT v5.3 inventory at a spatial resolution of 0.1° x 0.1° (Soulie et al., 2024), refined to the finest model resolution using land-use proxies (Mailler et al., 2017). Fire emissions came from the CAMS Global Fire Assimilation System (Kaiser et al., 2012). In this simulation, the BC emissions from Paris were specifically targeted. The BC Paris-to-regional ratio was calculated as $BC_{Paris}/(BC_{Paris}+BC_{regional})$, where BC_{Paris} and $BC_{regional}$ represent the BC concentrations coming from the Grand Paris domain (APUR, 2026) and the BC concentrations coming from the simulated regional background and boundary conditions, respectively (Di Antonio et al. 2023).

Forward trajectories were computed using the Hybrid Single Particle Lagrangian Integrated Trajectory model (HYSPLIT, Stein et al., 2015) with Global Data Assimilation System (GDAS) meteorological data as a complementary check for the physical link with the aircraft flight path. Trajectory calculations were performed at 1-hour intervals, with arrival heights corresponding to the aircraft altitude. The initial conditions were defined with respect to the geographic centre of Paris (48.86° North latitude and 2.34° East longitude). Air masses were then simulated forward in time in order to intersect the aircraft flight path at the corresponding sampling altitude and time.

2.3 Deriving intensive aerosol properties

The aerosol single scattering albedo ($SSA_{aer,\lambda}$) represents the balance between the scattering and the absorption of solar radiation by aerosols, providing insight into their potential to cool or warm the atmosphere. The $SSA_{aer,\lambda}$ was estimated using the following equation:

$$SSA_{aer,\lambda} = \frac{\sigma_{scatt,\lambda}}{\sigma_{ext,\lambda}} \quad \text{eq. (1)}$$

where σ_{ext} and σ_{scatt} represents the extinction and scattering coefficient at $\lambda = 450$ nm.

Yu et al. (2024) demonstrated that the difference between σ_{ext} and σ_{scatt} measured by the A2S2 can be used to estimate the absorption coefficient (σ_{abs}) from which the absorption Ångström Exponent (AAE) was calculated as follows:

$$AAE = -\frac{\log\left(\frac{\sigma_{abs,1}}{\sigma_{abs,2}}\right)}{\log\left(\frac{\lambda_1}{\lambda_2}\right)} \quad \text{eq. (2)}$$

where $\sigma_{abs,1}$ and $\sigma_{abs,2}$ represent the absorption coefficients at $\lambda_1 = 450$ nm and $\lambda_2 = 630$ nm, respectively.

The attribution of short-wavelength light absorption to BC and BrC has been achieved using the AAE. This method, well-established in the literature (Bergstrom et al., 2002; Kirchstetter et al., 2004; Bond and Bergstrom, 2006; Andreae and

https://doi.org/10.5194/egusphere-2026-4423
Preprint. Discussion started: 28 July 2026

Gelencsér, 2006; Lack and Langridge, 2013; Lu et al., 2015), utilises a pair of measurements spanning extremes of visible wavelength spectrum. Absorption at the longer wavelength (630 nm in this study) is assumed to be only due to BC and extrapolated to the shorter wavelength (450 nm), adopting a widely used AAE value of 1 (Bond et al., 2013). BrC absorption is then derived as the difference between the measured absorption and the BC-attributed absorption at the shorter wavelength, according to:

$$\sigma_{BrCabs,\lambda} = \sigma_{\text{abs},\lambda} - \sigma_{BCabs,\lambda} \quad \text{eq. (3)}$$

Different species ratios were derived from the relationships between aerosol and gas-phase concentrations to investigate the evolution of aerosol properties. The ΔOA/ΔBC ratio was calculated from the measurements of the mAMS and the SP2 as an indicator of SOA formation and atmospheric processing, while the ΔBC/ΔCO ratio served as indicator of amount and nature of sources. The $\Delta O_x/\Delta BC$ ratio (where $O_x = O_3+NO_2$) was used to assess shifts in the atmospheric oxidation state of the urban outflow (Liu, 1977; Wood et al., 2009; Canonaco et al., 2015; Wang et al., 2019; Thera et al., 2022; Yu et al., 2026a, b). Δ denotes an enhancement above background. Borbon et al., (2013) observed in the Paris plume during the MEGAPOLI experiment that C8 aromatics were more rapidly depleted by photochemical processing than toluene (e.g. ~17% after 30 min), highlighting their pronounced sensitivity to atmospheric oxidation. Thus, to assess the photochemical depletion of reactive volatile organic compounds, the C8 aromatics/toluene ratio was used. This ratio is also expected to decrease as photo-chemical age increases (Freney et al., 2014).

2.4 Estimation of outflow boundaries

Air masses were classified into urban and background categories following the criteria detailed in Velazquez-Garcia et al. (2026a). Briefly, urban and background air masses were initially defined as occurring when the mass concentration of BC exceeded the 75th percentile for a specific flight, whereas continental background conditions corresponded to concentrations below the 25th percentile (Table S1). This classification was subsequently validated by contrasting ΔBC/ΔCO emission ratios obtained for urban and background air masses (Figure 2b). The spatial extent of the urban plume for each flight was examined using WFR-CHIMERE simulations, alongside the BC Paris-to-regional ratio corresponding to the aircraft altitude. Figure 1 compares the observed BC mass concentration for a single flight (F28) with its respective simulated BC Paris-to-regional ratio. The urban plume exhibited coherent transport patterns, with peaks in BC concentrations occurring at locations that are consistent with the simulated plume cores, thereby supporting the attribution of these air masses to emissions originating from the Paris basin.

https://doi.org/10.5194/egusphere-2026-4423
Preprint. Discussion started: 28 July 2026

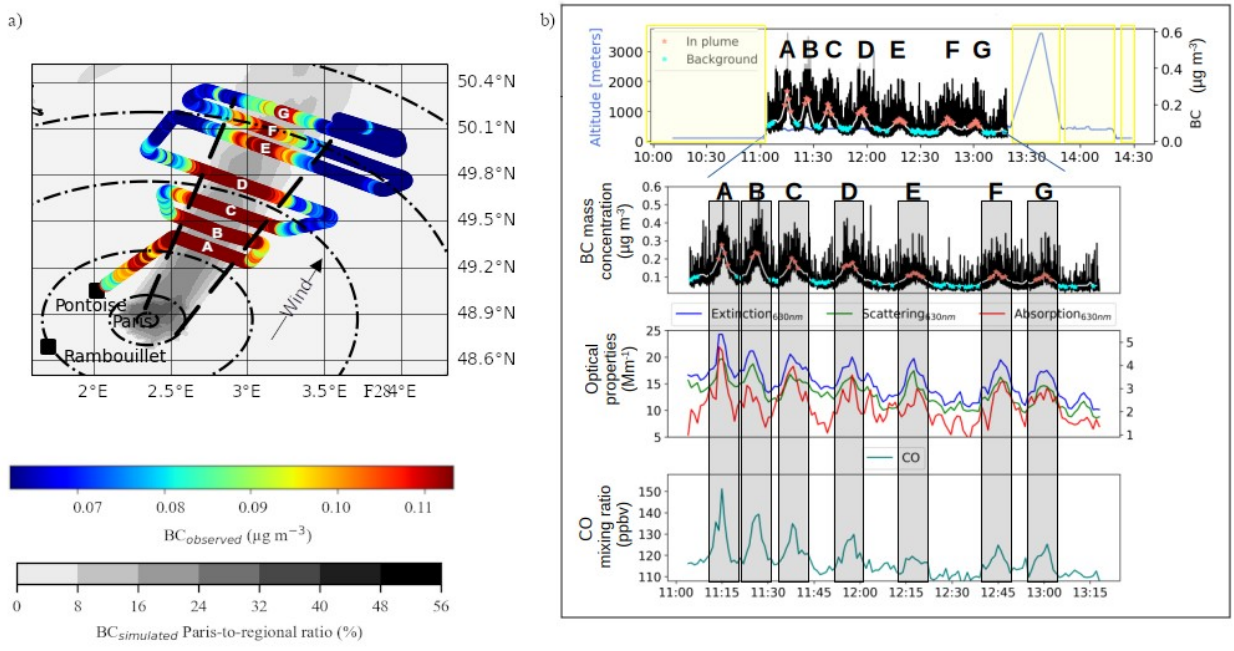

Figure 1. Plume identification. a) The left panel shows the spatial distribution along the flight track F28, illustrating the measured BC mass concentration (colour scale) overlaid on the WFR-CHIMERE-simulated Paris-to-regional BC ratio (grey-shaded contours). b) The right panel provides a magnified view of the time series of BC mass concentration, aerosol optical properties and CO mixing ratios. Red and blue stars along the BC time series mark the selected in plume and background conditions, respectively. Yellow-shaded areas indicate periods excluded from the analysis. Grey-shaded areas denote selected in-plume periods, defined by BC above the 75th percentile (letters A-G).

2.5 Determination of photochemical age (Δt)

The degree of photochemical processing (photochemical age, Δt) within the plume was estimated from hydrocarbon ratios, following previous studies (Borbon et al., 2013; de Gouw et al., 2005; Warneke et al., 2007). This calculation relates changes in VOC ratios to atmospheric ageing and allows extrapolation to a zero-photochemical-age condition. The photochemical age of an air mass can be calculated as follows:

$$\Delta t = \frac{1}{[OH]\left(k_{C8-aromatics} - k_{benzene}\right)} \times \left[\ln\left(\frac{[C8\,aromatics]}{[benzene]}\right)_{t=0} - \ln\left(\frac{[C8\,aromatics]}{[benzene]}\right)\right] \quad \text{eq. (4)}$$

where [OH] is the hydroxyl radical concentration assumed to be 5×10^{6} molec.cm^{-3} and $k_{C8\text{-romatics}}$ (1.4×10^{-11} cm^{3} molec^{-1} s^{-1}) and $k_{benzene}$ (1.22×10^{-12} cm^{3} molec^{-1} s^{-1}) are the reaction rate coefficients with OH for C8 aromatics and benzene respectively.

https://doi.org/10.5194/egusphere-2026-4423
Preprint. Discussion started: 28 July 2026

[benzene] and [C8 aromatics] are the mixing ratios in pptv of benzene and C8 aromatics, respectively. The concentration ratio at a photochemical age of zero was derived from a scatter plot of [C8 aromatics] vs [benzene] (Figure S1).

2.6 Statistical analyses

To explore the multivariate relationships driving the evolution of LACs within the Paris urban plume a Principal Component Analysis (PCA) was performed using key photochemical and compositional indicators. The selected features included the oxidation state tracers ($\Delta O_x/\Delta BC$, $\Delta OA/\Delta BC$), photochemical depletion (C8 aromatics/toluene), and the overall photochemical age retrieved. Due to the differing units and scales of the physical variables, the features were standardized to zero mean and unit variance using a StandardScaler prior to PCA implementation. The analysis computed all orthogonal principal components, with a particular focus on the primary components capturing the highest variance. The $AAE_{450\text{-}630nm}$ was explicitly excluded from the PCA matrix calculation and reserved as an independent control variable to validate the physical interpretation of the extracted components. To evaluate the relationship between plume ageing (represented by the dominant principal component) and the optical properties of BrC, a LOcally WEighted Scatterplot Smoothing (LOWESS) regression was applied with a smoothing fraction of 0.6.

3 Results and discussion

3.1 Variability in the contribution of carbonaceous aerosols to light absorption

Flights were conducted in all directions radiating from the centre of Paris to capture the urban plume's evolution as illustrated in Figure 2a. The flight strategy consisted of horizontal transects following the plume's flow at low altitudes – below 300 m above ground level – enabling a characterisation of the atmospheric boundary layer. The spatial distribution of BC mass concentration increased notably downwind of the city across the flights, consistent with the simulated Paris-to-regional BC ratio from the WRF-CHIMERE simulations. Figure 2b illustrates the relationship between BC mass concentration and CO mixing ratios. The contrasting slopes for the plume (3.4 ng m^{-3} ppb^{-1}) and background conditions (1.6 ng m^{-3} ppb^{-1}) demonstrate the successful identification of the Paris plume. Both values fall within the range of observations reported for urban plumes in previous studies (McMeeking et al., 2011; Spackman et al., 2008; Subramanian et al., 2010).

The analysis of σ_{abs} at 450 nm revealed differences in aerosol optical properties between plume and background conditions (Figure 2c). In both regimes, BC dominated light absorption, contributing more than 50% of the total absorption at 450 nm. The relative contribution of BrC was higher under background conditions (approximately 47%) than within the plume (approximately 38%). This difference was accompanied by slightly higher $SSA_{aer,450nm}$ values in background aerosols (median of 0.88 and 75th percentile of 0.91) compared with plume aerosols (median of 0.86 and 75th percentile of 0.89). Although small in magnitude, this shift is statistically significant (Mann–Whitney U test, $U = 7662.0$, $p < 0.005$), reflecting a more scattering-dominated aerosol population, a reduced dominance of BC absorption outside the plume and a larger influence of

https://doi.org/10.5194/egusphere-2026-4423
Preprint. Discussion started: 28 July 2026

OA-rich particles in the background atmosphere than in the plumes. Previous studies have reported similar relationships between increased scattering and enhanced aerosol AAE and higher OA fractions (Russell et al., 2010; Arola et al., 2011; Costabile et al., 2017; Velazquez-Garcia et al., 2023a; Di Antonio et al., 2025a; Pereira et al., 2025; Eom et al., 2025; Yu et al., 2026a, b).

There was notable variability in the BC/BrC ratio across different flight days within plume conditions (Figure S3). For instance, flight F29 showed the highest BC contribution (nearly 80%), whereas flight F34 exhibited a much stronger BrC influence, where BrC contributed roughly 60% to the total absorption. Flights with relatively larger BrC contributions tended to exhibit lower BC concentrations (Figure S4), corresponding to periods with lower overall pollution loading (Di Antonio et al., 2025a), suggesting that atmospheric processing altered the relative importance of absorbing aerosol components. This variability is consistent with the broader diversity in particle composition and ageing processes modulating the optical properties of urban plumes observed during the ACROSS campaign (Di Antonio et al., 2025a; Pereira et al., 2025; Yu et al., 2026a, b).

To further investigate the origins of BrC absorption, we examined the correlation between the ΔBC/ΔCO emission ratio and the BrC absorption (Figure S2). Inside the plume, a weak but statistically significant positive correlation was observed (Pearson coefficient R of 0.24, $p < 0.05$), indicating a detectable yet limited influence of plume emissions on BrC absorption. In contrast, no significant correlation was found under background conditions (Pearson coefficient R of -0.19, $p > 0.05$), suggesting that background BrC absorption was controlled by processes independent of those governing plume emissions. While prior research analysing biomass burning plumes have reported a distinct relationship between AAE and the ΔBC/ΔCO emission ratio – concluding that the absorption spectral dependence is modulated by burning conditions (Rupakheti et al., 2017; Selimovic et al., 2018, 2020; Che et al., 2022; Ding et al., 2023) – our data showed a weak correlation. This discrepancy indicated that the driving mechanism behind the BrC absorption in our study differs from primary combustions dynamics. Instead, this weak correlation suggested an alternative origin for the BrC contribution, which will be thoroughly examined in the subsequent sections.

https://doi.org/10.5194/egusphere-2026-4423
Preprint. Discussion started: 28 July 2026

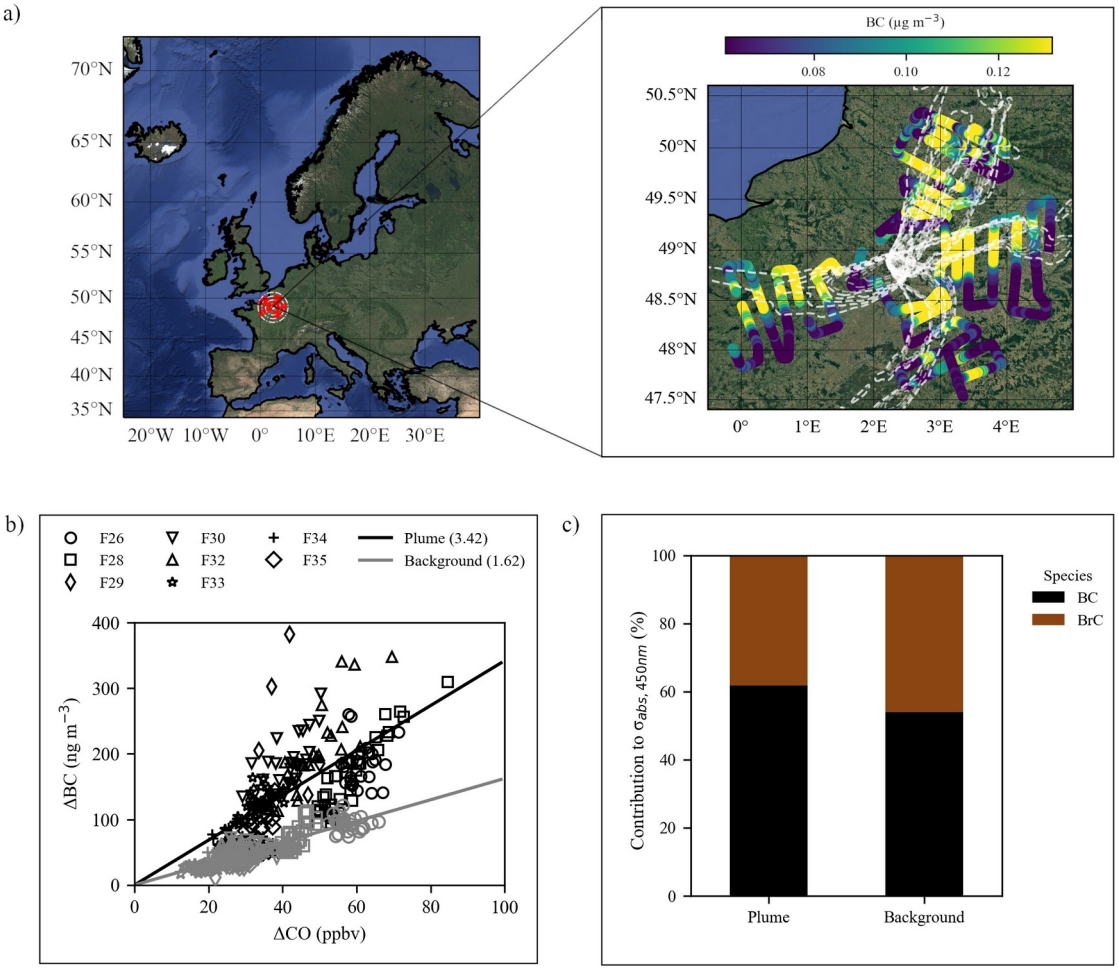

Figure 2. a) Geographic location of the ACROSS campaign. The left panel shows the overview map of Europe with the ATR42 flight patterns in red for altitudes below 300 m. The right panel displays a zoomed-in view of the flight tracks colour-coded by BC mass concentration, highlighting its spatial distribution. The white slashed lines represent the BC Paris-to-regional ratio simulated by the WRF-CHIMERE model. b) ΔBC/ΔCO emission ratio for in-plume (black) and background (gray) conditions with markers showing flight number and lines representing the linear regression. c) Contribution of BC and BrC to light absorption at 450 nm for in plume and background conditions.

3.2 Photochemical ageing within the Paris plume

Figure 3 illustrates the relationship between the evolution of O_x mixing ratio, normalised to BC within the urban plume, and the photochemical age estimated from eq. 4. A statistically significant, positive linear correlation is observed (Pearson coefficient R of 0.68, $p < 0.001$), with the $\Delta O_x/\Delta BC$ ratio increasing from approximately 35 to 50 ppbv μg^{-1} m^{-3} over a

https://doi.org/10.5194/egusphere-2026-4423
Preprint. Discussion started: 28 July 2026

photochemical lifetime of 12.5 hours. The oxidant production rate obtained from the slope of the linear fit suggested 1.2 ppbv of oxidants produced per µg m^{-3} of emitted BC per hour within the urban outflows intercepted during the ACROSS flights. The increase in $\Delta O_x/\Delta BC$ observed here at advanced photochemical ages suggests that oxidant production remains highly efficient throughout the plume's lifetime. Thera et al. (2022) reported CO-normalized oxidant production rates ranging from close to zero up to 0.27 ppb ppb^{-1} h^{-1} in the urban plumes of Paris measured during the MEGAPOLI campaign. Their study similarly showed that oxidant production remained active beyond 6 hours of transport, implying efficient photochemical production sustained by freshly emitted ozone precursors transported up to 200 km away from the Paris urban area. Likewise, Yu et al. (2026a, b) indicated that photo-chemical processing played a key role in O_x formation during the ACROSS campaign, with enhanced average $\Delta O_x/\Delta CO$ ratios in airborne observations of the urban plume relative to ground-based measurements in Paris.

Larger photochemical ageing during summer may result in enhanced VOCs consumption (Baudic et al., 2016; Borbon et al., 2013; Chen et al., 2021; Freney et al., 2014). Figure 3 shows the combined evolution of photochemical age, $\Delta O_x/\Delta BC$, and the C8 aromatics/toluene ratio in the urban plume. As indicated by the colour gradient, younger air masses (< 5 h) exhibit higher C8 aromatics/toluene ratios (>0.30 pptv $pptv^{-1}$, represented in yellow), consistent with a relatively fresh emissions signature. In contrast, at photochemical ages exceeding 7.5 h, the ratio decreases to below 0.20 pptv $pptv^{-1}$, reflecting the progressive depletion of C8 aromatic compounds relative to toluene.

Statistical analysis suggested that meteorological parameters exerted an influence on the $\Delta O_x/\Delta BC$ ratio (Figure S5). Temperature exhibited a significant positive correlation with the $\Delta O_x/\Delta BC$ ratio (Pearson coefficient R of 0.73, $p < 0.001$), reflecting the effect of boundary layer height, circulation patterns and solar-driven processes, as previously reported (Notario et al., 2013; Wang et al., 2013; Taheri et al., 2025; Pancholi et al., 2018; Pereira et al., 2025; Yu et al., 2026b; Baudic et al., 2016). In contrast, relative humidity displayed a weak, yet statistically significant, negative correlation with $\Delta O_x/\Delta BC$ (Pearson coefficient R of -0.29, $p < 0.001$). This inverse relationship is consistent with previous studies, which have shown that high relative humidity conditions can reduce photochemical activity through cloud-related attenuation of solar radiation and enhanced wet deposition, thereby limiting photochemical production rates (Mavroidis and Ilia, 2012; Pancholi et al., 2018; Song et al., 2011).

https://doi.org/10.5194/egusphere-2026-4423
Preprint. Discussion started: 28 July 2026

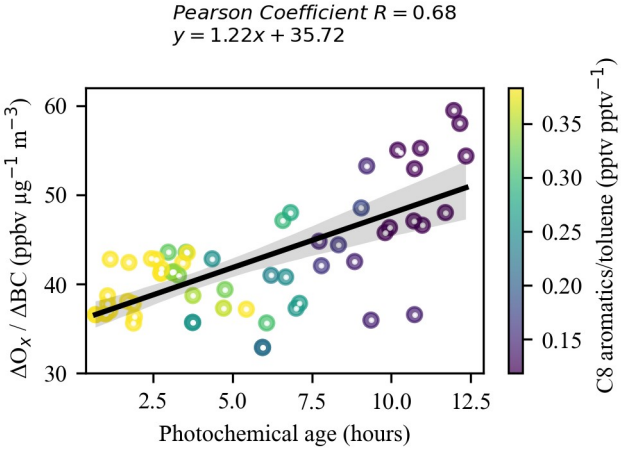

Figure 3. Total oxidant proxy normalised by BC as a function of photochemical age within the urban plume. The solid black line represents the linear regression fit (p-value < 0.001). Data points are colour-coded by the C8 aromatics/toluene ratio to illustrate the photochemical depletion of reactive VOCs.

335

3.3 Evolution of wavelength-dependent absorption with air mass oxidation

Figure 4 illustrates the changes of the aerosol composition and optical properties due to photochemical ageing. The link between air mass oxidation and organic aerosol production is reflected in the data, where $\Delta O_x/\Delta BC$ correlated significantly with $\Delta OA/\Delta BC$ (Pearson coefficient R of 0.71, $p < 0.001$). As the air mass becomes progressively more oxidised (moving 340 from lower to higher $\Delta O_x/\Delta BC$ bins), the $\Delta OA/\Delta BC$ ratio increased from approximately 3.7 to 5.5, suggesting enhanced organic aerosol production. This increase in OA mass was accompanied by an increase in photochemical age from 2.0 to 8.0 (Figure 4a). The C8 aromatics/toluene decreased with photochemical ageing, reflecting the photochemical consumption of anthropogenic VOCs (Figure 4b) as previously discussed. Similarly, the $AAE_{450–630nm}$ increased from 1.1 to 2.6 (Figure 4c), suggesting a growing contribution of light-absorbing organic material associated with ageing.

https://doi.org/10.5194/egusphere-2026-4423
Preprint. Discussion started: 28 July 2026

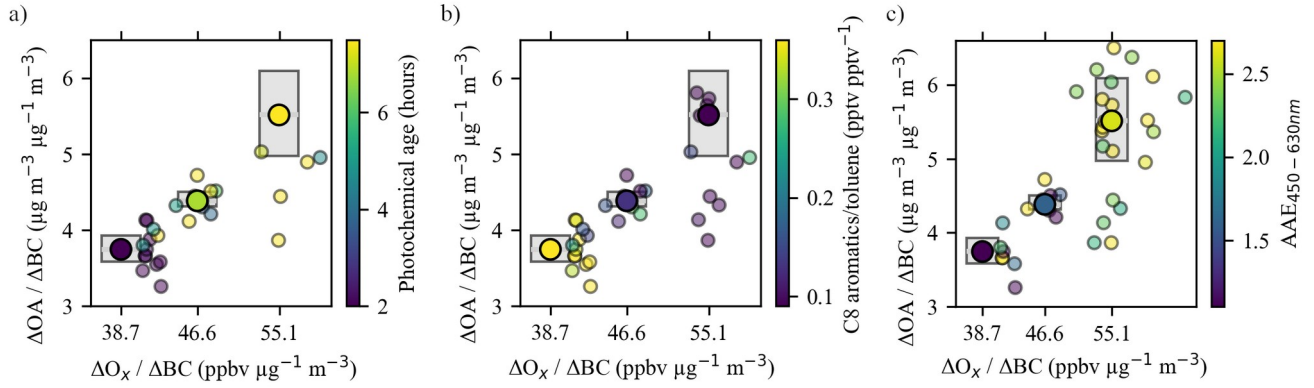

Figure 4. Evolution of aerosol chemical and optical properties as a function of oxidation state proxy bins. a) Organic aerosol enhancement as a function of plume age. b) Relationship between organic aerosol enhancement and the depletion of toluene. c) Enhancement the ΔOA/ΔBC ratio coloured by the Absorption Angstrom Exponent ($AAE_{450-630nm}$) mean values. The box plots represent the distribution of data points per each $\Delta O_x/\Delta BC$ bin.

The simultaneous increase in OA relative to BC and the depletion of toluene with ageing have been widely reported in previous studies of urban plumes (Borbon et al., 2013; Freney et al., 2014; McMeeking et al., 2011; Thera et al., 2022) and are commonly attributed to the oxidation of anthropogenic VOCs and their subsequent contribution to SOA formation during plume evolution. In addition, laboratory studies further support this interpretation, showing that the photo-oxidation of aromatic VOCs such as benzene, toluene, phenols, and polycyclic aromatic hydrocarbons (PAHs) in the presence of nitrogen oxides leads to the formation of light-absorbing secondary organic compounds, including nitro-aromatics (Flores et al., 2014; Lin et al., 2015). For instance, Nakayama et al., (2013) demonstrated that SOA formed from toluene photo-oxidation under varying NO_x conditions is dominated by nitro-aromatic species (e.g., nitrocresols), which strongly contribute to aerosol light absorption. Similarly, Teich et al. (2017) quantified significant contributions of nitrated aromatic compounds to the light absorption of ambient aerosol extracts collected in Germany and China. Pereira et al. (2025) showed positive correlations of O_3 with CHON compounds and negative correlations with CHOS in Paris, consistent with oxidative processing and the formation of nitrated organic species, which in urban environments are commonly associated with aromatic VOC oxidation in NO_x-rich plumes.

To statistically evaluate the changes in the optical properties of the aerosol during photochemical ageing, a Kruskal-Wallis test followed by a Dunn's post-hoc analysis was performed on the $AAE_{450–630nm}$ values grouped by the three distinct O_x/BC bins (Table S2). The global Kruskal-Wallis test indicated that the differences in AAE across the ageing groups were statistically significant ($p < 0.001$). Subsequent pairwise comparisons using Dunn's test revealed a highly significant difference in AAE between the lowest O_x/BC bin and the most evolutionarily advanced bin (55.1; $p < 0.001$). In contrast, the

https://doi.org/10.5194/egusphere-2026-4423
Preprint. Discussion started: 28 July 2026

differences between chronologically adjacent groups showed poor statistical significance, yielding p-values > 0.05. This statistical progression indicates that the cumulative photochemical ageing leads to a statistically distinct modification of the aerosol absorption characteristics between the initial and final stages of plume transport.

The PCA results (Figure S6 and Table S3) showed that PC1 was associated with plume processing, presenting high positive loadings on photochemical age (0.61) and $\Delta O_x/\Delta BC$ (0.44) along with negative loading on the C8 aromatics/toluene ratio (-0.59). In contrast, PC2 reflected variability in OA production as it is driven by a strong positive loading on the OA/ΔBC ratio (0.89). Together, these two components accounted for ~82% of the total atmospheric variance. Furthermore, the non-parametric LOWESS regression between the $AAE_{450\text{-}630nm}$ and the photochemical clock (PC1) revealed a non-monotonic upward trend that approached a plateau at advanced oxidation stages, despite the considerable variability among individual data points. At initial oxidation stages (PC1<0), low $AAE_{450\text{-}630nm}$ values (1.0-1.5) increased toward a plateau near 3.0, contributing to the overall evolutionary rate of 0.25 h^{-1} estimated from the binned $\Delta O_x/\Delta BC$ averages (Table S4). At advanced oxidation stages (PC1 >1) the $AAE_{450\text{-}630nm}$ appeared to stabilise, attributed to a potential balance between secondary production and photochemical loss of absorbing species, as has been suggested by previous studies (Laskin et al., 2015; Moise et al., 2015; Wong et al., 2017; Zhao et al., 2015). Nevertheless, given the limited data available in this extreme ageing regime, further research is needed to confirm this trend.

Overall, these results suggest that the observed "browning" of the Paris plume is driven by secondary organic aerosol formation. The increase in the ΔOA/ΔBC ratio with plume transport and increasing photochemical processing is consistent with the photochemical formation of BrC from precursor gases (e.g., aromatics). The concurrent increase in $AAE_{450\text{–}630nm}$ provides additional support for this interpretation, as higher AAE values are commonly associated with BrC. This interpretation also supports the trends observed by previous studies, demonstrating that the relative increase in BrC absorption can be attributed to active atmospheric chemistry producing new absorbing material (Di Antonio et al., 2025a; Pereira et al., 2025; Yu et al., 2026a, b). The depletion of C8 aromatics further supports this conclusion, as it serves as a proxy for the consumption of VOCs that act as SOA precursors in urban environments.

Previous studies investigating increases in AAE have identified the OA-to-BC ratio as a promising predictor of light absorption (Saleh et al., 2014; Bellouin, 2014; Moise et al., 2015; Lu et al., 2015; Costabile et al., 2017; McClure et al., 2020). Consistent with these observations, our results suggested a relationship between AAE and ΔOA/ΔBC, with a slope of d(AAE)/d(ΔOA/ΔBC) = 0.83 under the conditions examined here. The corresponding sensitivities for $\Delta O_x/\Delta BC$ and C8 aromatics/toluene were 0.091 and -0.0053, respectively (Table S4). This multi-parameter progression underscore the important role of anthropogenic SOA, such as nitrated aromatic compounds, on the optical footprint of urban plumes during transport.

https://doi.org/10.5194/egusphere-2026-4423
Preprint. Discussion started: 28 July 2026

4 Conclusions and implications

This study investigated the optical properties of light-absorbing carbonaceous aerosols within the Paris urban plume using airborne measurements conducted by the Safire ATR42 research aircraft during the ACROSS campaign. We derived an oxidant production rate of approximately 1.22 ppbv h^{-1} from the relationship between the oxidant mixing ratio normalised by BC and the photochemical clock. This increase in oxidant production was accompanied by the depletion of aromatic VOC precursors, providing evidence of active photochemical processing within the sampled urban plume. An observationally constrained AAE growth rate of 0.25 h^{-1} was derived over approximately 6 h of atmospheric processing, indicating a rapid increase in BrC absorption consistent with secondary aerosol formation during transport under the conditions encountered in this study. Our results suggest that photochemical ageing during plume transport promotes the formation of SOA from anthropogenic precursors and modifies aerosol optical properties, leading to higher SSA values and enhanced wavelength dependence of aerosol absorption.

Our observations are broadly consistent with previous laboratory, field, and modelling studies reporting photo-enhancement of BrC absorption through secondary formation processes followed by photobleaching at later stages of atmospheric aging (Zhao et al., 2015; Wang et al., 2019; Konovalov et al., 2021 and references herein). In particular, the observed increase in AAE together with the depletion of aromatic VOC precursors and increasing ΔOA/ΔBC ratios supports earlier evidence that anthropogenic aromatic oxidation can generate light-absorbing SOA. However, unlike most previous studies, which were conducted under laboratory conditions, at fixed surface sites, or focused on biomass-burning plumes, our airborne observations provide direct constraints on the coupled evolution of oxidation chemistry, SOA formation, and BrC optical properties within a real urban plume during transport. These results therefore extend current understanding of BrC ageing by demonstrating observationally that secondary formation processes can substantially enhance aerosol absorption on timescales of only a few hours in an anthropogenically influenced atmosphere.

Previous modelling studies that accounted for BrC ageing have shown improved simulations of aerosol light absorption (Park et al., 2010; Wang et al., 2014, 2018; Tuccella et al., 2025), but have primarily focused on the decline of absorption associated with photobleaching. Our findings suggest that representing BrC evolution solely through photobleaching may underestimate its contribution to aerosol absorption during the early stages of plume ageing, when secondary production of light-absorbing organic compounds is most active. Although the photobleaching in the latter stage could not be directly evaluated in our study because of the limited ageing times sampled during the campaign, this hypothesis highlights the need for observations spanning longer atmospheric processing times. More broadly, our study emphasises the importance of representing time-dependent changes in BrC absorption as a function of photochemical processing and aerosol composition, including variables such as ΔOA/ΔBC and SSA. Whether incorporating these observationally constrained processes into

https://doi.org/10.5194/egusphere-2026-4423
Preprint. Discussion started: 28 July 2026

atmospheric and climate models improves estimates of aerosol radiative effects and atmospheric heating rates in and around megacities remains to be evaluated.

Author contribution

Investigation: C. Denjean, C. Yu, S. Tinorua, T. Bourrianne, E. Arrufo, P. Di Carlo, P. F. DeCarlo, B. A. Nault, K. Tu, E. Pangui, D. L. Pereira, M. Cazaunau, A. Bauville, C. Cantrell, P. Formenti, V. Michoud. Methodology: A. Velazquez-Garcia, C. Denjean. Project administration: C. Denjean, M. Beekmann, C. Cantrell, P. Formenti, V. Michoud. Resources: H. Bouzidi, E. Arrufo, P. Di Carlo, L. Di Antonio, G. Siour, M. Beekmann, P. F. DeCarlo, B. A. Nault, P. Formenti, V. Michoud. Software: A. Velazquez-Garcia, S. Tinorua, L. Di Antonio, G. Siour, M. Beekmann. Supervision: C. Denjean. Validation: A. Velazquez-Garcia, C. Denjean. Visualization: A. Velazquez-Garcia Writing – original draft: A. Velazquez-Garcia. Writing – review & editing: A. Velazquez-Garcia and all co-authors

Acknowledgments

Airborne data was obtained using the aircraft managed by SAFIRE, the French Facility for airborne research, an infrastructure of the French National Center for Scientific Research (CNRS), Météo-France and the French National Center for Space Studies (CNES). The authors wish to thank AERIS (https://www.aeris-data.fr/, last access: 22/06/2026), the French centre for atmospheric data and service, for providing the campaign website and organising the curation and open distribution of the ACROSS data.

Funding

Airborne measurements using the Safire ATR-42 aircraft were supported by the ACROSS project, which benefits from French state aid (ANR – "Investissements d'avenir", grants n. ANR-17-MPGA-0002 and ANR-20-CE01-0010). The development of A252 instrument was funded by the Institut National des Sciences de l'Univers du Centre National de la Recherche Scientifique (INSU CNRS, grant no. AO-MILOURDS-INSU-2017). The modification and deployment of the HR-PTR-ToF-MS instrument have been performed with the support of the Technical Division of the INSU CNRS and have been supported by the "Ile de France" region in the framework of a call for projects from DIM QI2. A. Velazquez Garcia's work is supported by the CNRS (n° LS 220787) and Météo-France. C. Yu was supported by the Marie Skodowska-Curie COFUND Paris Regional Post-doctoral Fellowship program (grant n° 945298). The participation of P. De Carlo to the ACROSS field campaign was funded by the Invited Professor program of the University Paris Est.

Open Research

The dataset sampled with the Safire ATR42 research aircraft during the ACROSS field campaign and used in this study is available at the Aeris data centre. The SP2 data are accessible via Velazquez-Garcia et al. (2023b), the A2S2 data via Yu et al. (2023), the AMS data via Yu et al. (2024) and the HR-PTR-ToF-MS data via Michoud, V. & Bouzidi, H. (2024). CO, and

https://doi.org/10.5194/egusphere-2026-4423
Preprint. Discussion started: 28 July 2026

O_3 data are accessible via Cantrell C. (2023) and Cantrell C. (2024), respectively. The black carbon Paris-to-regional ratio modelling product is available via Di Antonio et al. (2023). All datasets are openly available upon registration.

Version 1.0.0 of the source codes used to process the SP2 data is preserved at Velazquez-Garcia et al. (2026). The code is openly available under an open source license and developed on GitHub.

Competing interests

At least one of the (co-)authors is a member of the editorial board of Atmospheric Chemistry and Physics.

References

Andreae, M. O. and Gelencsér, A.: Black carbon or brown carbon? The nature of light-absorbing carbonaceous aerosols, Atmospheric Chemistry and Physics, 6, 3131–3148, https://doi.org/10.5194/acp-6-3131-2006, 2006.

Arola, A., Schuster, G., Myhre, G., Kazadzis, S., Dey, S., and Tripathi, S. N.: Inferring absorbing organic carbon content from AERONET data, Atmospheric Chemistry and Physics, 11, 215–225, https://doi.org/10.5194/acp-11-215-2011, 2011.

Baudic, A., Gros, V., Sauvage, S., Locoge, N., Sanchez, O., Sarda-Estève, R., Kalogridis, C., Petit, J.-E., Bonnaire, N., Baisnée, D., Favez, O., Albinet, A., Sciare, J., and Bonsang, B.: Seasonal variability and source apportionment of volatile organic compounds (VOCs) in the Paris megacity (France), Atmospheric Chemistry and Physics, 16, 11961–11989, https://doi.org/10.5194/acp-16-11961-2016, 2016.

Bellouin, N.: The colour of smoke, Nature Geosci, 7, 619–620, https://doi.org/10.1038/ngeo2226, 2014.

Bergstrom, R. W., Russell, P. B., and Hignett, P.: Wavelength Dependence of the Absorption of Black Carbon Particles: Predictions and Results from the TARFOX Experiment and Implications for the Aerosol Single Scattering Albedo, Journal of the Atmospheric Sciences, 59, 567–577, https://doi.org/10.1175/1520-0469(2002)059%3C0567:WDOTAO%3E2.0.CO;2, 2002.

Bond, T. C. and Bergstrom, R. W.: Light Absorption by Carbonaceous Particles: An Investigative Review, Aerosol Science and Technology, 40, 27–67, https://doi.org/10.1080/02786820500421521, 2006.

Bond, T. C., Doherty, S. J., Fahey, D. W., Forster, P. M., Berntsen, T., DeAngelo, B. J., Flanner, M. G., Ghan, S., Kärcher, B., Koch, D., Kinne, S., Kondo, Y., Quinn, P. K., Sarofim, M. C., Schultz, M. G., Schulz, M., Venkataraman, C., Zhang, H., Zhang, S., Bellouin, N., Guttikunda, S. K., Hopke, P. K., Jacobson, M. Z., Kaiser, J. W., Klimont, Z., Lohmann, U., Schwarz, J. P., Shindell, D., Storelvmo, T., Warren, S. G., and Zender, C. S.: Bounding the role of black carbon in the climate system: A scientific assessment, Journal of Geophysical Research: Atmospheres, 118, 5380–5552, https://doi.org/10.1002/jgrd.50171, 2013.

Borbon, A., Gilman, J. B., Kuster, W. C., Grand, N., Chevaillier, S., Colomb, A., Dolgorouky, C., Gros, V., Lopez, M., Sarda-Esteve, R., Holloway, J., Stutz, J., Petetin, H., McKeen, S., Beekmann, M., Warneke, C., Parrish, D. D., and de Gouw, J. A.: Emission ratios of anthropogenic volatile organic compounds in northern mid-latitude megacities: Observations versus

https://doi.org/10.5194/egusphere-2026-4423
Preprint. Discussion started: 28 July 2026

emission inventories in Los Angeles and Paris, Journal of Geophysical Research: Atmospheres, 118, 2041–2057, https://doi.org/10.1002/jgrd.50059, 2013.

Canonaco, F., Slowik, J. G., Baltensperger, U., and Prévôt, A. S. H.: Seasonal differences in oxygenated organic aerosol composition: implications for emissions sources and factor analysis, Atmospheric Chemistry and Physics, 15, 6993–7002, https://doi.org/10.5194/acp-15-6993-2015, 2015.

Cantrell, C. and Michoud, V.: An Experiment to Study Atmospheric Oxidation Chemistry and Physics of Mixed Anthropogenic–Biogenic Air Masses in the Greater Paris Area, Bulletin of the American Meteorological Society, 103, 599–603, https://doi.org/10.1175/BAMS-D-21-0115.1, 2022.

Cantrell, C. ACROSS-2022_SAFIRE-ATR42_SAFIRE_CHEMISTRY-PICARRO_1MN CH4, CO2 and CO measurements. [Dataset]. Aeris. https://doi.org/10.25326/467, 2023.

Cantrell, C. ACROSS_ATR42_SAFIRE_CHEMISTRY_O3TEI49I_5SEC in situ measurements. [Dataset]. Aeris. https://doi.org/10.25326/629, 2024.

Che, H., Segal-Rozenhaimer, M., Zhang, L., Dang, C., Zuidema, P., Sedlacek III, A. J., Zhang, X., and Flynn, C.: Seasonal variations in fire conditions are important drivers in the trend of aerosol optical properties over the south-eastern Atlantic, Atmospheric Chemistry and Physics, 22, 8767–8785, https://doi.org/10.5194/acp-22-8767-2022, 2022.

Chen, T., Liu, J., Ma, Q., Chu, B., Zhang, P., Ma, J., Liu, Y., Zhong, C., Liu, P., Wang, Y., Mu, Y., and He, H.: Measurement report: Effects of photochemical aging on the formation and evolution of summertime secondary aerosol in Beijing, Atmospheric Chemistry and Physics, 21, 1341–1356, https://doi.org/10.5194/acp-21-1341-2021, 2021.

Corbin, J. C., Pieber, S. M., Czech, H., Zanatta, M., Jakobi, G., Massabò, D., Orasche, J., El Haddad, I., Mensah, A. A., Stengel, B., Drinovec, L., Mocnik, G., Zimmermann, R., Prévôt, A. S. H., and Gysel, M.: Brown and Black Carbon Emitted by a Marine Engine Operated on Heavy Fuel Oil and Distillate Fuels: Optical Properties, Size Distributions, and Emission Factors, Journal of Geophysical Research: Atmospheres, 123, 6175–6195, https://doi.org/10.1029/2017JD027818, 2018.

Corbin, J. C., Czech, H., Massabò, D., de Mongeot, F. B., Jakobi, G., Liu, F., Lobo, P., Mennucci, C., Mensah, A. A., Orasche, J., Pieber, S. M., Prévôt, A. S. H., Stengel, B., Tay, L.-L., Zanatta, M., Zimmermann, R., El Haddad, I., and Gysel, M.: Infrared-absorbing carbonaceous tar can dominate light absorption by marine-engine exhaust, npj Clim Atmos Sci, 2, 12, https://doi.org/10.1038/s41612-019-0069-5, 2019.

Costabile, F., Gilardoni, S., Barnaba, F., Di Ianni, A., Di Liberto, L., Dionisi, D., Manigrasso, M., Paglione, M., Poluzzi, V., Rinaldi, M., Facchini, M. C., and Gobbi, G. P.: Characteristics of brown carbon in the urban Po Valley atmosphere, Atmospheric Chemistry and Physics, 17, 313–326, https://doi.org/10.5194/acp-17-313-2017, 2017.

Denjean, C., Cassola, F., Mazzino, A., Triquet, S., Chevaillier, S., Grand, N., Bourrianne, T., Momboisse, G., Sellegri, K., Schwarzenbock, A., Freney, E., Mallet, M., and Formenti, P.: Size distribution and optical properties of mineral dust aerosols transported in the western Mediterranean, Atmospheric Chemistry and Physics, 16, 1081–1104, https://doi.org/10.5194/acp-16-1081-2016, 2016.

Desyaterik, Y., Sun, Y., Shen, X., Lee, T., Wang, X., Wang, T., and Collett Jr., J. L.: Speciation of "brown" carbon in cloud water impacted by agricultural biomass burning in eastern China, Journal of Geophysical Research: Atmospheres, 118, 7389–7399, https://doi.org/10.1002/jgrd.50561, 2013.

https://doi.org/10.5194/egusphere-2026-4423
Preprint. Discussion started: 28 July 2026

Di Antonio, L., Siour, G. & Beekmann, M. ACROSS_LISA_CHIMERE_BCRatio_1H. [Dataset]. Aeris. https://doi.org/10.25326/529, 2023.

Di Antonio, L., Di Biagio, C., Formenti, P., Gratien, A., Michoud, V., Cantrell, C., Bauville, A., Bergé, A., Cazaunau, M., Chevaillier, S., Cirtog, M., Coll, P., D'Anna, B., de Brito, J. F., De Haan, D. O., Dignum, J. R., Deshmukh, S., Favez, O., Flaud, P.-M., Gaimoz, C., Hawkins, L. N., Kammer, J., Language, B., Maisonneuve, F., Močnik, G., Perraudin, E., Petit, J.-E., Acharja, P., Poulain, L., Pouyes, P., Pronovost, E. D., Riffault, V., Roundtree, K. I., Shahin, M., Siour, G., Villenave, E., Zapf, P., Foret, G., Doussin, J.-F., and Beekmann, M.: Aerosol spectral optical properties in the Paris urban area and its peri-urban and forested surroundings during summer 2022 from ACROSS surface observations, Atmospheric Chemistry and Physics, 25, 3161–3189, https://doi.org/10.5194/acp-25-3161-2025, 2025a.

Di Antonio, L., Beekmann, M., Siour, G., Michoud, V., Cantrell, C., Bauville, A., Bergé, A., Cazaunau, M., Chevaillier, S., Cirtog, M., de Brito, J. F., Formenti, P., Gaimoz, C., Garret, O., Gratien, A., Gros, V., Haeffelin, M., Hawkins, L. N., Kotthaus, S., Noyalet, G., Pereira, D. L., Petit, J.-E., Pronovost, E. D., Riffault, V., Yu, C., Foret, G., Doussin, J.-F., and Di Biagio, C.: Modelling of atmospheric variability in gas and aerosols during the ACROSS campaign 2022 of the greater Paris area: evaluation of the meteorology, dynamics and chemistry, Atmospheric Chemistry and Physics, 25, 4803–4831, https://doi.org/10.5194/acp-25-4803-2025, 2025b.

Di Carlo, P., Aruffo, E., Busilacchio, M., Giammaria, F., Dari-Salisburgo, C., Biancofiore, F., Visconti, G., Lee, J., Moller, S., Reeves, C. E., Bauguitte, S., Forster, G., Jones, R. L., and Ouyang, B.: Aircraft based four-channel thermal dissociation laser induced fluorescence instrument for simultaneous measurements of NO_2, total peroxy nitrate, total alkyl nitrate, and HNO_3, Atmospheric Measurement Techniques, 6, 971–980, https://doi.org/10.5194/amt-6-971-2013, 2013.

Ding, S., Liu, D., Zhao, D., Tian, P., Huang, M., and Ding, D.: Characteristics of atmospheric black carbon and its wet scavenging in Nanning, South China, Science of The Total Environment, 904, 166747, https://doi.org/10.1016/j.scitotenv.2023.166747, 2023.

Dingle, J. H., Zimmerman, S., Frie, A. L., Min, J., Jung, H., and Bahreini, R.: Complex refractive index, single scattering albedo, and mass absorption coefficient of secondary organic aerosols generated from oxidation of biogenic and anthropogenic precursors, Aerosol Science and Technology, 53, 449–463, https://doi.org/10.1080/02786826.2019.1571680, 2019.

Drewnick, F., Hings, S. S., DeCarlo, P., Jayne, J. T., Gonin, M., Fuhrer, K., Weimer, S., Jimenez, J. L., Demerjian, K. L., Borrmann, S., and Worsnop, D. R.: A New Time-of-Flight Aerosol Mass Spectrometer (TOF-AMS)—Instrument Description and First Field Deployment, Aerosol Science and Technology, 39, 637–658, https://doi.org/10.1080/02786820500182040, 2005.

Drugé, T., Nabat, P., Mallet, M., Michou, M., Rémy, S., and Dubovik, O.: Modeling radiative and climatic effects of brown carbon aerosols with the ARPEGE-Climat global climate model, Atmospheric Chemistry and Physics, 22, 12167–12205, https://doi.org/10.5194/acp-22-12167-2022, 2022.

Eom, S., Park, S. S., Liu, X., Oxford, C. R., Martin, R. V., Kim, J., and Song, C.-K.: Impact of Chemical Composition on Aerosol Scattering: Insights from the Surface Particulate Matter Network and Aerosol Robotic Network, Environ. Sci. Technol., 59, 19899–19909, https://doi.org/10.1021/acs.est.5c09325, 2025.

APUR: https://opendata.apur.org/datasets/Apur::etablissements-publics-territoriaux-metropole-du-grand-paris/, last access: 10 June 2026.

https://doi.org/10.5194/egusphere-2026-4423
Preprint. Discussion started: 28 July 2026

Feng, Y., Ramanathan, V., and Kotamarthi, V. R.: Brown carbon: a significant atmospheric absorber of solar radiation?, Atmospheric Chemistry and Physics, 13, 8607–8621, https://doi.org/10.5194/acp-13-8607-2013, 2013.

Filges, A., Gerbig, C., Chen, H., Franke, H., Klaus, C., and Jordan, A.: The IAGOS-core greenhouse gas package: a measurement system for continuous airborne observations of CO2, CH4, H2O and CO, Tellus B: Chemical and Physical Meteorology, 67, 27989, https://doi.org/10.3402/tellusb.v67.27989, 2015.

Flores, J. M., Washenfelder, R. A., Adler, G., Lee, H. J., Segev, L., Laskin, J., Laskin, A., Nizkorodov, S. A., Brown, S. S., and Rudich, Y.: Complex refractive indices in the near-ultraviolet spectral region of biogenic secondary organic aerosol aged with ammonia, Phys. Chem. Chem. Phys., 16, 10629–10642, https://doi.org/10.1039/C4CP01009D, 2014.

Formenti, P., Rajot, J. L., Desboeufs, K., Saïd, F., Grand, N., Chevaillier, S., and Schmechtig, C.: Airborne observations of mineral dust over western Africa in the summer Monsoon season: spatial and vertical variability of physico-chemical and optical properties, Atmospheric Chemistry and Physics, 11, 6387–6410, https://doi.org/10.5194/acp-11-6387-2011, 2011.

Forrister, H., Liu, J., Scheuer, E., Dibb, J., Ziemba, L., Thornhill, K. L., Anderson, B., Diskin, G., Perring, A. E., Schwarz, J. P., Campuzano-Jost, P., Day, D. A., Palm, B. B., Jimenez, J. L., Nenes, A., and Weber, R. J.: Evolution of brown carbon in wildfire plumes, Geophysical Research Letters, 42, 4623–4630, https://doi.org/10.1002/2015GL063897, 2015.

Freney, E. J., Sellegri, K., Canonaco, F., Colomb, A., Borbon, A., Michoud, V., Doussin, J.-F., Crumeyrolle, S., Amarouche, N., Pichon, J.-M., Bourianne, T., Gomes, L., Prevot, A. S. H., Beekmann, M., and Schwarzenböeck, A.: Characterizing the impact of urban emissions on regional aerosol particles: airborne measurements during the MEGAPOLI experiment, Atmospheric Chemistry and Physics, 14, 1397–1412, https://doi.org/10.5194/acp-14-1397-2014, 2014.

Gliß, J., Mortier, A., Schulz, M., Andrews, E., Balkanski, Y., Bauer, S. E., Benedictow, A. M. K., Bian, H., Checa-Garcia, R., Chin, M., Ginoux, P., Griesfeller, J. J., Heckel, A., Kipling, Z., Kirkevåg, A., Kokkola, H., Laj, P., Le Sager, P., Lund, M. T., Lund Myhre, C., Matsui, H., Myhre, G., Neubauer, D., van Noije, T., North, P., Olivié, D. J. L., Rémy, S., Sogacheva, L., Takemura, T., Tsigaridis, K., and Tsyro, S. G.: AeroCom phase III multi-model evaluation of the aerosol life cycle and optical properties using ground- and space-based remote sensing as well as surface in situ observations, Atmospheric Chemistry and Physics, 21, 87–128, https://doi.org/10.5194/acp-21-87-2021, 2021.

de Gouw, J. A., Middlebrook, A. M., Warneke, C., Goldan, P. D., Kuster, W. C., Roberts, J. M., Fehsenfeld, F. C., Worsnop, D. R., Canagaratna, M. R., Pszenny, A. a. P., Keene, W. C., Marchewka, M., Bertman, S. B., and Bates, T. S.: Budget of organic carbon in a polluted atmosphere: Results from the New England Air Quality Study in 2002, Journal of Geophysical Research: Atmospheres, 110, https://doi.org/10.1029/2004JD005623, 2005.

Hems, R. F. and Abbatt, J. P. D.: Aqueous Phase Photo-oxidation of Brown Carbon Nitrophenols: Reaction Kinetics, Mechanism, and Evolution of Light Absorption, ACS Earth and Space Chemistry, 2, 225–234, https://doi.org/10.1021/acsearthspacechem.7b00123, 2018.

Jacobson, M. Z.: Isolating nitrated and aromatic aerosols and nitrated aromatic gases as sources of ultraviolet light absorption, Journal of Geophysical Research: Atmospheres, 104, 3527–3542, https://doi.org/10.1029/1998JD100054, 1999.

Kaiser, J. W., Heil, A., Andreae, M. O., Benedetti, A., Chubarova, N., Jones, L., Morcrette, J.-J., Razinger, M., Schultz, M. G., Suttie, M., and van der Werf, G. R.: Biomass burning emissions estimated with a global fire assimilation system based on observed fire radiative power, Biogeosciences, 9, 527–554, https://doi.org/10.5194/bg-9-527-2012, 2012.

https://doi.org/10.5194/egusphere-2026-4423
Preprint. Discussion started: 28 July 2026

Kaskaoutis, D. G., Liakakou, E., Grivas, G., Gerasopoulos, E., Mihalopoulos, N., Alastuey, A., Dulac, F., Dumka, U. C., Pandolfi, M., Pikridas, M., Sciare, J., and Titos, G.: Interannual Variability and Long-Term Trends of Aerosols Above the Mediterranean, in: Atmospheric Chemistry in the Mediterranean Region: Volume 1 - Background Information and Pollutant Distribution, edited by: Dulac, F., Sauvage, S., and Hamonou, E., Springer International Publishing, Cham, 357–390, https://doi.org/10.1007/978-3-031-12741-0_11, 2023.

Kirchstetter, T. W., Novakov, T., and Hobbs, P. V.: Evidence that the spectral dependence of light absorption by aerosols is affected by organic carbon, Journal of Geophysical Research: Atmospheres, 109, https://doi.org/10.1029/2004JD004999, 2004.

Konovalov, I. B., Golovushkin, N. A., Beekmann, M., and Andreae, M. O.: Insights into the aging of biomass burning aerosol from satellite observations and 3D atmospheric modeling: evolution of the aerosol optical properties in Siberian wildfire plumes, Atmospheric Chemistry and Physics, 21, 357–392, https://doi.org/10.5194/acp-21-357-2021, 2021.

Konwar, M., Werden, B., Fortner, E. C., Bera, S., Varghese, M., Chowdhuri, S., Hibert, K., Croteau, P., Jayne, J., Canagaratna, M., Malap, N., Jayakumar, S., Dixit, S. A., Murugavel, P., Axisa, D., Baumgardner, D., DeCarlo, P. F., Worsnop, D. R., and Prabhakaran, T.: Identifying the seeding signature in cloud particles from hydrometeor residuals, Atmospheric Measurement Techniques, 17, 2387–2400, https://doi.org/10.5194/amt-17-2387-2024, 2024.

Laborde, M., Mertes, P., Zieger, P., Dommen, J., Baltensperger, U., and Gysel, M.: Sensitivity of the Single Particle Soot Photometer to different black carbon types, Atmospheric Measurement Techniques, 5, 1031–1043, https://doi.org/10.5194/amt-5-1031-2012, 2012.

Lack, D. A. and Langridge, J. M.: On the attribution of black and brown carbon light absorption using the Ångström exponent, Atmospheric Chemistry and Physics, 13, 10535–10543, https://doi.org/10.5194/acp-13-10535-2013, 2013.

Laskin, A., Laskin, J., and Nizkorodov, S. A.: Chemistry of Atmospheric Brown Carbon, Chemical Reviews, 115, 4335–4382, https://doi.org/10.1021/cr5006167, 2015.

Lee, H. J. (Julie), Aiona, P. K., Laskin, A., Laskin, J., and Nizkorodov, S. A.: Effect of Solar Radiation on the Optical Properties and Molecular Composition of Laboratory Proxies of Atmospheric Brown Carbon, Environ. Sci. Technol., 48, 10217–10226, https://doi.org/10.1021/es502515r, 2014.

Li, J., Carlson, B. E., Yung, Y. L., Lv, D., Hansen, J., Penner, J. E., Liao, H., Ramaswamy, V., Kahn, R. A., Zhang, P., Dubovik, O., Ding, A., Lacis, A. A., Zhang, L., and Dong, Y.: Scattering and absorbing aerosols in the climate system, Nat Rev Earth Environ, 3, 363–379, https://doi.org/10.1038/s43017-022-00296-7, 2022.

Lin, P., Laskin, J., Nizkorodov, S. A., and Laskin, A.: Revealing Brown Carbon Chromophores Produced in Reactions of Methylglyoxal with Ammonium Sulfate, Environ. Sci. Technol., 49, 14257–14266, https://doi.org/10.1021/acs.est.5b03608, 2015.

Liu, P. F., Abdelmalki, N., Hung, H.-M., Wang, Y., Brune, W. H., and Martin, S. T.: Ultraviolet and visible complex refractive indices of secondary organic material produced by photooxidation of the aromatic compounds toluene and *m*-xylene, Atmospheric Chemistry and Physics, 15, 1435–1446, https://doi.org/10.5194/acp-15-1435-2015, 2015.

Liu, S. C.: Possible effects on fropospheric O 3 and OH due to No emissions, Geophysical Research Letters, 4, 325–328, https://doi.org/10.1029/GL004i008p00325, 1977.

https://doi.org/10.5194/egusphere-2026-4423
Preprint. Discussion started: 28 July 2026

Lu, Z., Streets, D. G., Winijkul, E., Yan, F., Chen, Y., Bond, T. C., Feng, Y., Dubey, M. K., Liu, S., Pinto, J. P., and Carmichael, G. R.: Light Absorption Properties and Radiative Effects of Primary Organic Aerosol Emissions, Environ. Sci. Technol., 49, 4868–4877, https://doi.org/10.1021/acs.est.5b00211, 2015.

Mailler, S., Menut, L., Khvorostyanov, D., Valari, M., Couvidat, F., Siour, G., Turquety, S., Briant, R., Tuccella, P., Bessagnet, B., Colette, A., Létinois, L., Markakis, K., and Meleux, F.: CHIMERE-2017: from urban to hemispheric chemistry-transport modeling, Geoscientific Model Development, 10, 2397–2423, https://doi.org/10.5194/gmd-10-2397-2017, 2017.

Mavroidis, I. and Ilia, M.: Trends of NOx, NO2 and O3 concentrations at three different types of air quality monitoring stations in Athens, Greece, Atmospheric Environment, 63, 135–147, https://doi.org/10.1016/j.atmosenv.2012.09.030, 2012.

McClure, C. D., Lim, C. Y., Hagan, D. H., Kroll, J. H., and Cappa, C. D.: Biomass-burning-derived particles from a wide variety of fuels – Part 1: Properties of primary particles, Atmospheric Chemistry and Physics, 20, 1531–1547, https://doi.org/10.5194/acp-20-1531-2020, 2020.

McMeeking, G. R., Morgan, W. T., Flynn, M., Highwood, E. J., Turnbull, K., Haywood, J., and Coe, H.: Black carbon aerosol mixing state, organic aerosols and aerosol optical properties over the United Kingdom, Atmospheric Chemistry and Physics, 11, 9037–9052, https://doi.org/10.5194/acp-11-9037-2011, 2011.

Menut, L., Bessagnet, B., Briant, R., Cholakian, A., Couvidat, F., Mailler, S., Pennel, R., Siour, G., Tuccella, P., Turquety, S., and Valari, M.: The CHIMERE v2020r1 online chemistry-transport model, Geoscientific Model Development Discussions, 1–50, https://doi.org/10.5194/gmd-2021-96, 2021.

Michoud, V. & Bouzidi, H. ACROSS_LISA_SAFIRE-ATR42_PTRMS-VOCs_20220617-20220705. [Dataset]. Aeris. https://doi.org/10.25326/654, 2024.

Moise, T., Flores, J. M., and Rudich, Y.: Optical Properties of Secondary Organic Aerosols and Their Changes by Chemical Processes, Chemical Reviews, 115, 4400–4439, https://doi.org/10.1021/cr5005259, 2015.

Moteki, N. and Kondo, Y.: Dependence of Laser-Induced Incandescence on Physical Properties of Black Carbon Aerosols: Measurements and Theoretical Interpretation, Aerosol Science and Technology, 44, 663–675, https://doi.org/10.1080/02786826.2010.484450, 2010.

Nakayama, T., Sato, K., Matsumi, Y., Imamura, T., Yamazaki, A., and Uchiyama, A.: Wavelength and NO_x dependent complex refractive index of SOAs generated from the photooxidation of toluene, Atmospheric Chemistry and Physics, 13, 531–545, https://doi.org/10.5194/acp-13-531-2013, 2013.

Navarro-Barboza, H., Rovira, J., Obiso, V., Pozzer, A., Via, M., Alastuey, A., Querol, X., Perez, N., Savadkoohi, M., Chen, G., Yus-Díez, J., Ivancic, M., Rigler, M., Eleftheriadis, K., Vratolis, S., Zografou, O., Gini, M., Chazeau, B., Marchand, N., Prevot, A. S. H., Dallenbach, K., Ehn, M., Luoma, K., Petäjä, T., Tobler, A., Necki, J., Aurela, M., Timonen, H., Niemi, J., Favez, O., Petit, J.-E., Putaud, J.-P., Hueglin, C., Pascal, N., Chauvigné, A., Conil, S., Pandolfi, M., and Jorba, O.: Characterization of brown carbon absorption in different European environments through source contribution analysis, Atmospheric Chemistry and Physics, 25, 2667–2694, https://doi.org/10.5194/acp-25-2667-2025, 2025.

Notario, A., Bravo, I., Adame, J. A., Díaz-de-Mera, Y., Aranda, A., Rodríguez, A., and Rodríguez, D.: Partitioning, sources and variability of regional and local oxidant (OX = O3 + NO2) in a coastal rural area in the southwest of Iberian Peninsula, Environ Sci Pollut Res, 20, 6059–6069, https://doi.org/10.1007/s11356-013-1642-9, 2013.

https://doi.org/10.5194/egusphere-2026-4423
Preprint. Discussion started: 28 July 2026

Pancholi, P., Kumar, A., Bikundia, D. S., and Chourasiya, S.: An observation of seasonal and diurnal behavior of O3–NOx relationships and local/regional oxidant (OX = O3 + NO2) levels at a semi-arid urban site of western India, Sustainable Environment Research, 28, 79–89, https://doi.org/10.1016/j.serj.2017.11.001, 2018.

Park, R. J., Kim, M. J., Jeong, J. I., Youn, D., and Kim, S.: A contribution of brown carbon aerosol to the aerosol light absorption and its radiative forcing in East Asia, Atmospheric Environment, 44, 1414–1421, https://doi.org/10.1016/j.atmosenv.2010.01.042, 2010.

Pereira, D. L., Giorio, C., Gratien, A., Zherebker, A., Noyalet, G., Chevaillier, S., Alage, S., Almarj, E., Bergé, A., Bertin, T., Cazaunau, M., Coll, P., Di Antonio, L., Harb, S., Heuser, J., Gaimoz, C., Guillemant, O., Language, B., Lauret, O., Macias, C., Maisonneuve, F., Picquet-Varrault, B., Torres, R., Triquet, S., Zapf, P., Hawkins, L., Pronovost, D., Riley, S., Flaud, P.-M., Perraudin, E., Pouyes, P., Villenave, E., Albinet, A., Favez, O., Aujay-Plouzeau, R., Michoud, V., Cantrell, C., Cirtog, M., Di Biagio, C., Doussin, J.-F., and Formenti, P.: Molecular characterization of organic aerosols in urban and forested areas of Paris using high-resolution mass spectrometry, Atmospheric Chemistry and Physics, 25, 4885–4905, https://doi.org/10.5194/acp-25-4885-2025, 2025.

Rupakheti, D., Adhikary, B., Praveen, P. S., Rupakheti, M., Kang, S., Mahata, K. S., Naja, M., Zhang, Q., Panday, A. K., and Lawrence, M. G.: Pre-monsoon air quality over Lumbini, a world heritage site along the Himalayan foothills, Atmospheric Chemistry and Physics, 17, 11041–11063, https://doi.org/10.5194/acp-17-11041-2017, 2017.

Russell, P. B., Bergstrom, R. W., Shinozuka, Y., Clarke, A. D., DeCarlo, P. F., Jimenez, J. L., Livingston, J. M., Redemann, J., Dubovik, O., and Strawa, A.: Absorption Angstrom Exponent in AERONET and related data as an indicator of aerosol composition, Atmospheric Chemistry and Physics, 10, 1155–1169, https://doi.org/10.5194/acp-10-1155-2010, 2010.

Saleh, R.: From Measurements to Models: Toward Accurate Representation of Brown Carbon in Climate Calculations, Current Pollution Reports, 6, 90–104, https://doi.org/10.1007/s40726-020-00139-3, 2020.

Saleh, R., Hennigan, C. J., McMeeking, G. R., Chuang, W. K., Robinson, E. S., Coe, H., Donahue, N. M., and Robinson, A. L.: Absorptivity of brown carbon in fresh and photo-chemically aged biomass-burning emissions, Atmospheric Chemistry and Physics, 13, 7683–7693, https://doi.org/10.5194/acp-13-7683-2013, 2013.

Saleh, R., Robinson, E. S., Tkacik, D. S., Ahern, A. T., Liu, S., Aiken, A. C., Sullivan, R. C., Presto, A. A., Dubey, M. K., Yokelson, R. J., Donahue, N. M., and Robinson, A. L.: Brownness of organics in aerosols from biomass burning linked to their black carbon content, Nature Geosci, 7, 647–650, https://doi.org/10.1038/ngeo2220, 2014.

Samset, B. H., Stjern, C. W., Andrews, E., Kahn, R. A., Myhre, G., Schulz, M., and Schuster, G. L.: Aerosol Absorption: Progress Towards Global and Regional Constraints, Curr Clim Change Rep, 4, 65–83, https://doi.org/10.1007/s40641-018-0091-4, 2018.

Sareen, N., Moussa, S. G., and McNeill, V. F.: Photochemical Aging of Light-Absorbing Secondary Organic Aerosol Material, J. Phys. Chem. A, 117, 2987–2996, https://doi.org/10.1021/jp309413j, 2013.

Schwarz, J. P., Gao, R. S., Spackman, J. R., Watts, L. A., Thomson, D. S., Fahey, D. W., Ryerson, T. B., Peischl, J., Holloway, J. S., Trainer, M., Frost, G. J., Baynard, T., Lack, D. A., de Gouw, J. A., Warneke, C., and Del Negro, L. A.: Measurement of the mixing state, mass, and optical size of individual black carbon particles in urban and biomass burning emissions, Geophysical Research Letters, 35, https://doi.org/10.1029/2008GL033968, 2008.

https://doi.org/10.5194/egusphere-2026-4423
Preprint. Discussion started: 28 July 2026

Selimovic, V., Yokelson, R. J., Warneke, C., Roberts, J. M., de Gouw, J., Reardon, J., and Griffith, D. W. T.: Aerosol optical properties and trace gas emissions by PAX and OP-FTIR for laboratory-simulated western US wildfires during FIREX, Atmospheric Chemistry and Physics, 18, 2929–2948, https://doi.org/10.5194/acp-18-2929-2018, 2018.

Selimovic, V., Yokelson, R. J., McMeeking, G. R., and Coefield, S.: Aerosol Mass and Optical Properties, Smoke Influence on O3, and High NO3 Production Rates in a Western U.S. City Impacted by Wildfires, Journal of Geophysical Research: Atmospheres, 125, e2020JD032791, https://doi.org/10.1029/2020JD032791, 2020.

Song, F., Young Shin, J., Jusino-Atresino, R., and Gao, Y.: Relationships among the springtime ground–level NOx, O3 and NO3 in the vicinity of highways in the US East Coast, Atmospheric Pollution Research, 2, 374–383, https://doi.org/10.5094/APR.2011.042, 2011.

Soulie, A., Granier, C., Darras, S., Zilbermann, N., Doumbia, T., Guevara, M., Jalkanen, J.-P., Keita, S., Liousse, C., Crippa, M., Guizzardi, D., Hoesly, R., and Smith, S. J.: Global anthropogenic emissions (CAMS-GLOB-ANT) for the Copernicus Atmosphere Monitoring Service simulations of air quality forecasts and reanalyses, Earth System Science Data, 16, 2261–2279, https://doi.org/10.5194/essd-16-2261-2024, 2024.

Spackman, J. R., Schwarz, J. P., Gao, R. S., Watts, L. A., Thomson, D. S., Fahey, D. W., Holloway, J. S., de Gouw, J. A., Trainer, M., and Ryerson, T. B.: Empirical correlations between black carbon aerosol and carbon monoxide in the lower and middle troposphere, Geophysical Research Letters, 35, https://doi.org/10.1029/2008GL035237, 2008.

Stein, A. F., Draxler, R. R., Rolph, G. D., Stunder, B. J. B., Cohen, M. D., and Ngan, F.: NOAA's HYSPLIT Atmospheric Transport and Dispersion Modeling System, Bulletin of the American Meteorological Society, 96, 2059–2077, https://doi.org/10.1175/BAMS-D-14-00110.1, 2015.

Subramanian, R., Kok, G. L., Baumgardner, D., Clarke, A., Shinozuka, Y., Campos, T. L., Heizer, C. G., Stephens, B. B., de Foy, B., Voss, P. B., and Zaveri, R. A.: Black carbon over Mexico: the effect of atmospheric transport on mixing state, mass absorption cross-section, and BC/CO ratios, Atmospheric Chemistry and Physics, 10, 219–237, https://doi.org/10.5194/acp-10-219-2010, 2010.

Szopa, S., Naik, V., Adhikary, B., and Artaxo, P.: Short-Lived Climate Forcers. In Climate Change 2021: The Physical Science Basis. Contribution of Working Group I to the Sixth Assessment Report of the Intergovernmental Panel on Climate Change, 1st ed., Cambridge University Press, Cambridge, United Kingdom and New York, NY, USA, 817–922 pp., https://doi.org/10.1017/9781009157896, 2023.

Taheri, A., Khorsandi, B., and Alavi Moghaddam, M. R.: A long-term analysis of oxidant (OX = O3 + NO2) and its local and regional levels in Tehran, Iran, a high NOx-saturated condition, Sci Rep, 15, 2521, https://doi.org/10.1038/s41598-024-82709-9, 2025.

Teich, M., van Pinxteren, D., Wang, M., Kecorius, S., Wang, Z., Müller, T., Močnik, G., and Herrmann, H.: Contributions of nitrated aromatic compounds to the light absorption of water-soluble and particulate brown carbon in different atmospheric environments in Germany and China, Atmospheric Chemistry and Physics, 17, 1653–1672, https://doi.org/10.5194/acp-17-1653-2017, 2017.

Thera, B., Dominutti, P., Colomb, A., Michoud, V., Doussin, J.-F., Beekmann, M., Dulac, F., Sartelet, K., and Borbon, A.: O 3 –NO y photochemistry in boundary layer polluted plumes: insights from the MEGAPOLI (Paris), ChArMEx/SAFMED (North West Mediterranean) and DACCIWA (southern West Africa) aircraft campaigns, Environmental Science: Atmospheres, 2, 659–686, https://doi.org/10.1039/D1EA00093D, 2022.

https://doi.org/10.5194/egusphere-2026-4423
Preprint. Discussion started: 28 July 2026

Tinorua, S., Denjean, C., Nabat, P., Bourrianne, T., Pont, V., Gheusi, F., and Leclerc, E.: Higher absorption enhancement of black carbon in summer shown by 2-year measurements at the high-altitude mountain site of Pic du Midi Observatory in the French Pyrenees, Atmospheric Chemistry and Physics, 24, 1801–1824, https://doi.org/10.5194/acp-24-1801-2024, 2024.

Tuccella, P., Di Antonio, L., Di Muzio, A., Colaiuda, V., Lidori, R., Menut, L., Pitari, G., and Raparelli, E.: Modeling the Black and Brown Carbon Absorption and Their Radiative Impact: The June 2023 Intense Canadian Boreal Wildfires Case Study, Journal of Geophysical Research: Atmospheres, 130, e2024JD042674, https://doi.org/10.1029/2024JD042674, 2025.

Velazquez-Garcia, A., Crumeyrolle, S., de Brito, J. F., Tison, E., Bourrianne, E., Chiapello, I., and Riffault, V.: Deriving composition-dependent aerosol absorption, scattering and extinction mass efficiencies from multi-annual high time resolution observations in Northern France, Atmospheric Environment, 298, 119613, https://doi.org/10.1016/j.atmosenv.2023.119613, 2023a.

Velazquez-Garcia, A., Denjean, C., Tinorua, S., & Bourriane, T. ACROSS_CNRM_SAFIRE -ATR42_rBC [Dataset]. Aeris. https://doi.org/10.25326/504, 2023b.

Velazquez-Garcia, A., de Brito, J. F., Crumeyrolle, S., Chiapello, I., and Riffault, V.: Assessment of light-absorbing carbonaceous aerosol origins and properties at the ATOLL site in northern France, Aerosol Research, 2, 107–122, https://doi.org/10.5194/ar-2-107-2024, 2024.

Velazquez-Garcia, A., Denjean, C., Yu, C., Tinorua, S., Bourrianne, T., Burnet, F., Tu, K., Pangui, E., Pereira, D. L., Cazaunau, M., Di Antonio, L., Siour, G., Beekmann, M., DeCarlo, P. F., Nault, B. A., Bauville, A., Cantrell, C., Formenti, P., and Michoud, V.: Observational Evidence for Relative Humidity Driving Black Carbon Mixing State and Absorption Enhancement in Urban Outflows, Geophysical Research Letters, 53, e2025GL121520, https://doi.org/10.1029/2025GL121520, 2026a.

Velazquez-Garcia, A., Tinorua, S. & Denjean, C. SP2Py-Proo-toolkit-and-codes-to-produce-manuscript-s-figures. [Software]. Zenodo. https://doi.org/10.5281/zenodo.18185577, 2026b.

Vu, K. T., Dingle, J. H., Bahreini, R., Reddy, P. J., Apel, E. C., Campos, T. L., DiGangi, J. P., Diskin, G. S., Fried, A., Herndon, S. C., Hills, A. J., Hornbrook, R. S., Huey, G., Kaser, L., Montzka, D. D., Nowak, J. B., Pusede, S. E., Richter, D., Roscioli, J. R., Sachse, G. W., Shertz, S., Stell, M., Tanner, D., Tyndall, G. S., Walega, J., Weibring, P., Weinheimer, A. J., Pfister, G., and Flocke, F.: Impacts of the Denver Cyclone on regional air quality and aerosol formation in the Colorado Front Range during FRAPPÉ 2014, Atmospheric Chemistry and Physics, 16, 12039–12058, https://doi.org/10.5194/acp-16-12039-2016, 2016.

W. Kirchstetter, T., Harley, R. A., Kreisberg, N. M., Stolzenburg, M. R., and Hering, S. V.: On-road measurement of fine particle and nitrogen oxide emissions from light- and heavy-duty motor vehicles, Atmospheric Environment, 33, 2955–2968, https://doi.org/10.1016/S1352-2310(99)00089-8, 1999.

Wang, Q., Han, Y., Ye, J., Liu, S., Pongpiachan, S., Zhang, N., Han, Y., Tian, J., Wu, C., Long, X., Zhang, Q., Zhang, W., Zhao, Z., and Cao, J.: High Contribution of Secondary Brown Carbon to Aerosol Light Absorption in the Southeastern Margin of Tibetan Plateau, Geophysical Research Letters, 46, 4962–4970, https://doi.org/10.1029/2019GL082731, 2019.

Wang, X., Heald, C. L., Ridley, D. A., Schwarz, J. P., Spackman, J. R., Perring, A. E., Coe, H., Liu, D., and Clarke, A. D.: Exploiting simultaneous observational constraints on mass and absorption to estimate the global direct radiative forcing of black carbon and brown carbon, Atmospheric Chemistry and Physics, 14, 10989–11010, https://doi.org/10.5194/acp-14-10989-2014, 2014.

https://doi.org/10.5194/egusphere-2026-4423
Preprint. Discussion started: 28 July 2026

Wang, X., Heald, C. L., Sedlacek, A. J., de Sá, S. S., Martin, S. T., Alexander, M. L., Watson, T. B., Aiken, A. C., Springston, S. R., and Artaxo, P.: Deriving brown carbon from multiwavelength absorption measurements: method and application to AERONET and Aethalometer observations, Atmospheric Chemistry and Physics, 16, 12733–12752, https://doi.org/10.5194/acp-16-12733-2016, 2016.

Wang, X., Heald, C. L., Liu, J., Weber, R. J., Campuzano-Jost, P., Jimenez, J. L., Schwarz, J. P., and Perring, A. E.: Exploring the observational constraints on the simulation of brown carbon, Atmospheric Chemistry and Physics, 18, 635–653, https://doi.org/10.5194/acp-18-635-2018, 2018.

Wang, Y., Hu, B., Tang, G., Ji, D., Zhang, H., Bai, J., Wang, X., and Wang, Y.: Characteristics of ozone and its precursors in Northern China: A comparative study of three sites, Atmospheric Research, 132–133, 450–459, https://doi.org/10.1016/j.atmosres.2013.04.005, 2013.

Warneke, C., McKeen, S. A., de Gouw, J. A., Goldan, P. D., Kuster, W. C., Holloway, J. S., Williams, E. J., Lerner, B. M., Parrish, D. D., Trainer, M., Fehsenfeld, F. C., Kato, S., Atlas, E. L., Baker, A., and Blake, D. R.: Determination of urban volatile organic compound emission ratios and comparison with an emissions database, Journal of Geophysical Research: Atmospheres, 112, https://doi.org/10.1029/2006JD007930, 2007.

Washenfelder, R. A., Attwood, A. R., Brock, C. A., Guo, H., Xu, L., Weber, R. J., Ng, N. L., Allen, H. M., Ayres, B. R., Baumann, K., Cohen, R. C., Draper, D. C., Duffey, K. C., Edgerton, E., Fry, J. L., Hu, W. W., Jimenez, J. L., Palm, B. B., Romer, P., Stone, E. A., Wooldridge, P. J., and Brown, S. S.: Biomass burning dominates brown carbon absorption in the rural southeastern United States, Geophysical Research Letters, 42, 653–664, https://doi.org/10.1002/2014GL062444, 2015.

Wong, J. P. S., Nenes, A., and Weber, R. J.: Changes in Light Absorptivity of Molecular Weight Separated Brown Carbon Due to Photolytic Aging, Environmental Science & Technology, 51, 8414–8421, https://doi.org/10.1021/acs.est.7b01739, 2017.

Wong, J. P. S., Tsagkaraki, M., Tsiodra, I., Mihalopoulos, N., Violaki, K., Kanakidou, M., Sciare, J., Nenes, A., and Weber, R. J.: Atmospheric evolution of molecular-weight-separated brown carbon from biomass burning, Atmospheric Chemistry and Physics, 19, 7319–7334, https://doi.org/10.5194/acp-19-7319-2019, 2019.

Wood, E. C., Herndon, S. C., Onasch, T. B., Kroll, J. H., Canagaratna, M. R., Kolb, C. E., Worsnop, D. R., Neuman, J. A., Seila, R., Zavala, M., and Knighton, W. B.: A case study of ozone production, nitrogen oxides, and the radical budget in Mexico City, Atmospheric Chemistry and Physics, 9, 2499–2516, https://doi.org/10.5194/acp-9-2499-2009, 2009.

Xie, C., Xu, W., Wang, J., Wang, Q., Liu, D., Tang, G., Chen, P., Du, W., Zhao, J., Zhang, Y., Zhou, W., Han, T., Bian, Q., Li, J., Fu, P., Wang, Z., Ge, X., Allan, J., Coe, H., and Sun, Y.: Vertical characterization of aerosol optical properties and brown carbon in winter in urban Beijing, China, Atmospheric Chemistry and Physics, 19, 165–179, https://doi.org/10.5194/acp-19-165-2019, 2019.

Yu, C., & Formenti, P. ACROSS_LISA_SAFIRE-ATR42_A2S2-Ext-Scatt-450_20220618-20220705 [Dataset]. Aeris. https://doi.org/10.25326/526, 2023.

Yu, C., DeCarlo, P., Nault, B., & Formenti, P. ACROSS_LISA_SAFIRE -ATR42_AMS_20220618 -20220705 [Dataset]. Aeris. https://doi.org/10.25326/686, 2024.

Yu, C., Pangui, E., Tu, K., Cazaunau, M., Feingesicht, M., Xavier, L., Bourrianne, T., Michoud, V., Cantrell, C., Onasch, T. B., Freedman, A., and Formenti, P.: Characterisation of particle single-scattering albedo with a modified airborne dual-

https://doi.org/10.5194/egusphere-2026-4423
Preprint. Discussion started: 28 July 2026

wavelength CAPS monitor, Atmospheric Measurement Techniques, 17, 3419–3437, https://doi.org/10.5194/amt-17-3419-2024, 2024.

Yu, C., Formenti, P., de Brito, J. F., Bauville, A., Bergé, A., Bouzidi, H., Cazaunau, M., Cirtog, M., Di Biagio, C., Di Antonio, L., Gaimoz, C., Maisonneuve, F., Zapf, P., Seubert, T., Andersen, S. T., Dewald, P., Türk, G. N. T. E., Crowley, J. N., Kukui, A., Xue, C., Denjean, C., Garrouste, O., Etienne, J.-C., Wu, H., Allan, J. D., Liu, D., Wu, Y., Cantrell, C., and Michoud, V.: Impacts of summertime photochemical aging on the physicochemical properties of aerosols in a Paris suburban forest region, Atmospheric Chemistry and Physics, 26, 5313–5332, https://doi.org/10.5194/acp-26-5313-2026, 2026a.

Yu, C., Di Antonio, L., DeCarlo, P. F., Nault, B. A., Velazquez-Garcia, A., Aruffo, E., Di Carlo, P., Denjean, C., Tinorua, S., Bourrianne, T., Pereira, D. L., Tu, K., Pangui, E., Cazaunau, M., Bauville, A., Grand, N., Bergé, A., Di Biagio, C., Gratien, A., Beekmann, M., Siour, G., Foret, G., D'Anna, B., Kammer, J., Wu, H., Cantrell, C., Formenti, P., and Michoud, V.: Evolution of aerosol composition and optical properties in the Paris urban plume from coordinated airborne and ground-based observations, EGUsphere, 1–34, https://doi.org/10.5194/egusphere-2026-3147, 2026b.

Zhang, X., Lin, Y.-H., Surratt, J. D., Zotter, P., Prévôt, A. S. H., and Weber, R. J.: Light-absorbing soluble organic aerosol in Los Angeles and Atlanta: A contrast in secondary organic aerosol, Geophysical Research Letters, 38, https://doi.org/10.1029/2011GL049385, 2011.

Zhang, Y., Forrister, H., Liu, J., Dibb, J., Anderson, B., Schwarz, J. P., Perring, A. E., Jimenez, J. L., Campuzano-Jost, P., Wang, Y., Nenes, A., and Weber, R. J.: Top-of-atmosphere radiative forcing affected by brown carbon in the upper troposphere, Nature Geosci, 10, 486–489, https://doi.org/10.1038/ngeo2960, 2017.

Zhao, R., Lee, A. K. Y., Huang, L., Li, X., Yang, F., and Abbatt, J. P. D.: Photochemical processing of aqueous atmospheric brown carbon, Atmospheric Chemistry and Physics, 15, 6087–6100, https://doi.org/10.5194/acp-15-6087-2015, 2015.

Zhong, M. and Jang, M.: Dynamic light absorption of biomass-burning organic carbon photochemically aged under natural sunlight, Atmospheric Chemistry and Physics, 14, 1517–1525, https://doi.org/10.5194/acp-14-1517-2014, 2014.